nature neuroscience

BRIEF COMMUNICATION

https://doi.org/10.1038/s41593-019-0421-4

Morphine withdrawal recruits lateral habenula cytokine signaling to reduce synaptic excitation and sociability

Kristina Valentinova[1,2,6], Anna Tchenio[1,6], Massimo Trusel[1], Joseph A. Clerke[1], Arnaud L. Lalive[1], Stamatina Tzanoulinou[3], Alessandro Matera[4], Imane Moutkine[5], Luc Maroteaux[5], Rosa C. Paolicelli[4], Andrea Volterra[1], Camilla Bellone[3] and Manuel Mameli[1,5*]

The lateral habenula encodes aversive stimuli contributing to negative emotional states during drug withdrawal. Here we report that morphine withdrawal in mice leads to microglia adaptations and diminishes glutamatergic transmission onto raphe-projecting lateral habenula neurons. Chemogenetic inhibition of this circuit promotes morphine withdrawal-like social deficits. Morphine withdrawal-driven synaptic plasticity and reduced sociability require tumor necrosis factor-α (TNF-α) release and neuronal TNF receptor 1 activation. Hence, habenular cytokines control synaptic and behavioral adaptations during drug withdrawal.

Opiate withdrawal produces negative states, including low mood and reduced sociability, which contribute to relapse during drug abstinence[1,2]. Dysfunction of the lateral habenula (LHb)—a nucleus that controls monoaminergic systems and processes aversive stimuli—underlies depressive symptoms typical of drug withdrawal[3]; however, how opiates affect the LHb remains poorly understood[4,5].

We subjected mice to naloxone-precipitated morphine withdrawal (MORwd) to examine its repercussions on glutamatergic synapses onto LHb neurons[1]. Indeed, aberrant LHb excitatory transmission underlies negative symptoms in rodent models of depression and addiction[3]. Spontaneous excitatory postsynaptic current (sEPSC) amplitudes, but not frequencies, were reduced only in LHb neurons located in the medial aspect (^{Med}LHb; Supplementary Fig. 1a–b). Accordingly, MORwd diminished AMPA receptor (AMPAR)/NMDA receptor (NMDAR) ratios solely in the ^{Med}LHb (Fig. 1a; Supplementary Fig. 1c) without affecting neurotransmitter release, as assessed via trains of synaptic stimulation (Supplementary Fig. 1d). Recordings obtained 1 h after the last morphine injection (without naloxone) yielded saline-comparable AMPAR/NMDAR ratios. In contrast, spontaneous MORwd decreased AMPAR/NMDAR ratios in the ^{Med}LHb up to 30 days after the last morphine injection (Supplementary Fig. 1e).

To assess whether MORwd affects AMPAR conductance or number, we analyzed peak-scaled non-stationary fluctuations of ^{Med}LHb-recorded sEPSCs[6]. While single-channel conductance remained unaffected in MORwd slices, the number of channels opened at the peak was positively correlated with amplitude values (Supplementary Fig. 1f). MORwd failed to alter AMPAR-EPSC rectification (Supplementary Fig. 1g), whereas it reduced glutamate

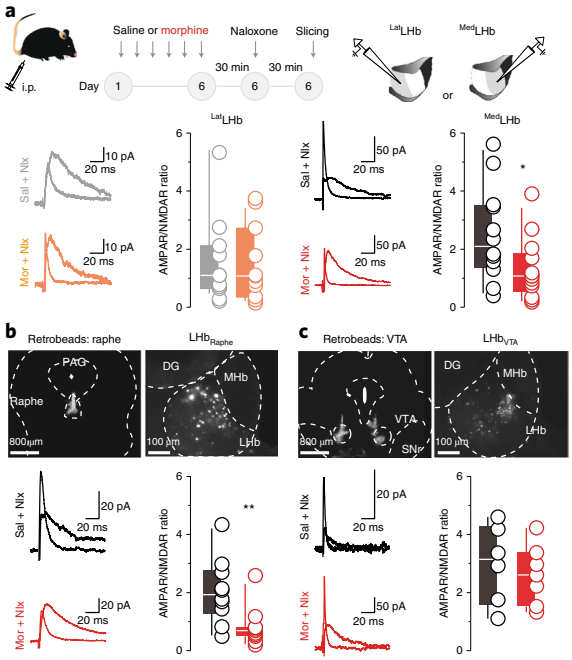

Fig. 1 | MORwd-driven projection-specific synaptic depression in the LHb. **a**, Top: naloxone-precipitated MORwd (NP-MORwd) protocol. Bottom left: traces and AMPAR/NMDAR ratios from ^{Lat}LHb slices (saline + naloxone (Sal+Nlx; $n = 7$ mice, 11 cells) versus NP-MORwd (Mor+Nlx; $n = 8$ mice, 11 cells)). Two-sided t test, $t_{20} = 0.0548$, $P = 0.957$. Bottom right: traces and AMPAR/NMDAR ratios from ^{Med}LHb slices (saline + naloxone ($n = 7$ mice, 12 cells) versus NP-MORwd ($n = 8$ mice, 13 cells)). Two-sided t test, $t_{23} = 2.210$, $^{*}P = 0.037$. i.p., intraperitoneal injection. **b**, Top: images of retrobeads in raphe and retrogradely labeled LHb_{Raphe} neurons. Bottom: Traces and AMPAR/NMDAR ratios from LHb_{Raphe} neurons (saline + naloxone ($n = 5$ mice, 10 cells) versus NP-MORwd ($n = 5$ mice, 11 cells)). Two-sided t test, $t_{19} = 3.153$, $^{**}P = 0.005$. **c**, Same as **b**, but in LHb_{VTA} neurons (saline + naloxone ($n = 2$ mice, 6 cells) versus NP-MORwd ($n = 4$ mice, 7 cells)). Two-sided t test, $t_{11} = 0.575$, $P = 0.577$. PAG, periaqueductal gray; DG, dentate gyrus; MHb, medial habenula; SNr, substantia nigra pars reticulata. Data are presented as box plots, with 10th and 90th percentiles, median and scatter.

[1]The Department of Fundamental Neuroscience, The University of Lausanne, Lausanne, Switzerland. [2]Department of Physiology, The University of Bern, Bern, Switzerland. [3]Department of Basic Neuroscience, The University of Geneva, Geneva, Switzerland. [4]Department of Physiology, The University of Lausanne, Lausanne, Switzerland. [5]Inserm, UMR-S 839, Paris, France. [6]These authors contributed equally: Kristina Valentinova and Anna Tchenio. *e-mail: manuel.mameli@unil.ch

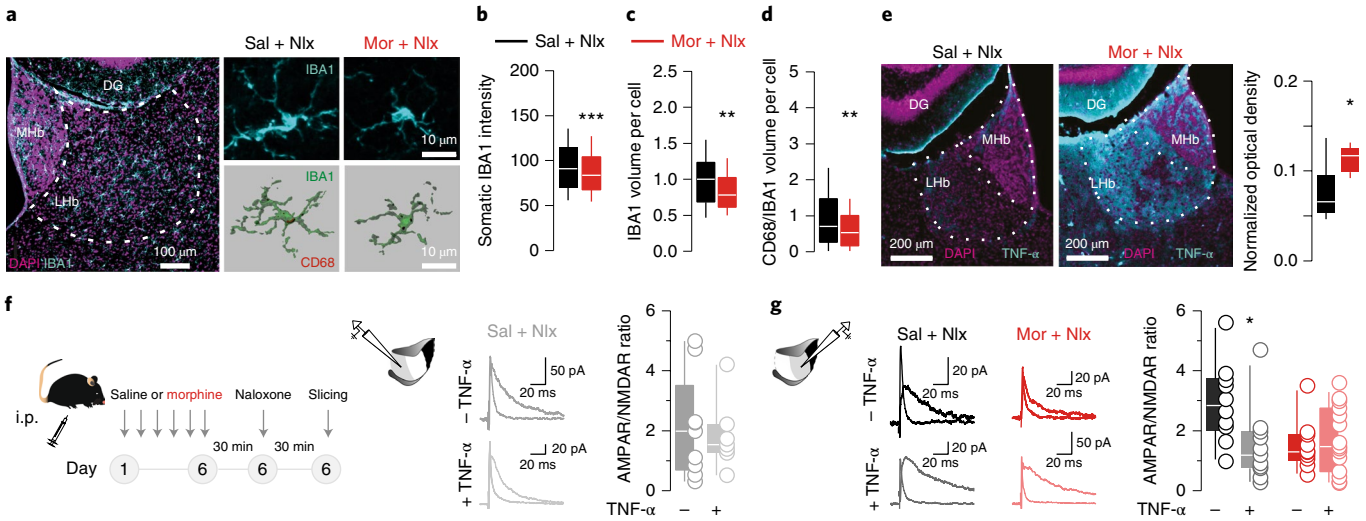

Fig. 2 | Cytokine signaling in the LHb for MORwd plasticity. a, Max-projection of confocal image of the LHb with IBA1$^+$ microglia (left). Max-projection of ^{Med}LHb microglia in saline + naloxone and NP-MORwd mice (upper right). 3D reconstruction of IBA1$^+$ microglia containing CD68 structures from slices obtained from saline + naloxone and NP-MORwd mice (lower right). **b**, Analysis of IBA1 microglia immunoreactivity in ^{Med}LHb slices (saline + naloxone ($n = 4$ mice, 366 cells), NP-MORwd ($n = 4$ mice, 328 cells)). Two-sided t test, $t_{692} = 3.305$, $^{***}P = 0.001$; 3 independent acquisition sessions. **c**,**d**, Quantitative analyses of microglial cell volume (based on IBA1 immunoreactivity) and CD68$^+$ structures. Values are normalized to saline control (saline + naloxone (black; $n_{mice/cells} = 4$ mice, 89 cells), NP-MORwd (red; $n = 4$ mice, 83 cells)). IBA1 volume (**c**): two-sided t test, $t_{170} = 3.05$, $^{**}P = 0.003$. CD68/IBA1 volume (**d**): two-sided t test, $t_{170} = 2.65$, $^{**}P = 0.008$. Measurements were obtained from independent samples. **e**, TNF-α (cyan) and DAPI (magenta) immunostaining and normalized TNF-α optical density in the LHb (saline + naloxone (black; $n = 7$ mice, 6 independent acquisitions per mouse) versus NP-MORwd (red; $n = 8$ mice, 5 independent acquisitions per mouse)). Two-sided t test, $t_{13} = 2.991$, $^{*}P = 0.0104$. **f**, Experimental protocol (left) and example traces and AMPAR/NMDAR ratios (right) in the ^{Lat}LHb with (+) or without (–) exogenous TNF-α (saline + naloxone –TNF-α ($n = 2$ mice, 9 cells) versus saline + naloxone +TNF-α ($n = 2$ mice, 9 cells)). Two-sided t test, $t_{14} = 0.37$, $P = 0.717$. **g**, AMPAR/NMDAR ratios with or without exogenous TNF-α recorded from saline + naloxone ($n = 3$ mice, 10 cells (–TNF-α) and $n = 4$ mice, 11 cells (+TNF-α)) and NP-MORwd ^{Med}LHb slices ($n = 3$ mice, 10 cells (–TNF-α) and $n = 5$ mice, 15 cells (+TNF-α)). Interaction factor $F_{(1,42)} = 4.90$, two-way ANOVA, $^{*}P = 0.039$. Data are presented as box plots, with 10th and 90th percentiles, median and scatter.

uncaging-evoked AMPAR/NMDAR ratios, yielding a decrease only in absolute AMPAR currents (Supplementary Fig. 1h). This suggests that MORwd reduces, in a territory-specific fashion, the number of AMPARs without affecting their biophysical properties, NMDAR numbers or presynaptic glutamate release.

MORwd-evoked plasticity occurs onto ^{Med}LHb neurons, which innervate downstream structures, including the raphe nucleus and the ventral tegmental area (VTA)[7]. MORwd diminished AMPAR/NMDAR ratios solely in retrobead-labeled raphe-projecting (LHb_{Raphe}) but not VTA-projecting LHb (LHb_{VTA}) neurons (Fig. 1b,c). These results point to the specificity of MORwd for discrete habenular circuits.

Which induction mechanism gates MORwd-driven plasticity onto ^{Med}LHb neurons? Inflammatory responses and glial cell activation emerge during drug withdrawal[8]. Indeed, spontaneous MORwd drives microglia adaptations and pro-inflammatory cytokine release (that is, TNF-α)[9]. Notably, cocaine also leads to reduced microglia arborization along with TNF-α-dependent AMPAR internalization, which partly underlies drug-mediated behavioral adaptations[8]. We found that within the ^{Med}LHb, MORwd reduced microglial markers, including IBA1 and CD68, and diminished microglial cell volume (Fig. 2a–d). In parallel, naloxone-induced and spontaneous MORwd increased habenular TNF-α immunolabeling (Fig. 2e; Supplementary Fig. 2a–d). Altogether, these findings support the view that there is engagement of inflammatory responses and cytokine signaling within the LHb during MORwd.

We then reasoned that if MORwd promotes TNF-α release, artificially increasing its levels should prove sufficient to recapitulate MORwd-driven synaptic plasticity. Incubating LHb-containing slices obtained from saline-injected mice with exogenous TNF-α reduced AMPAR/NMDAR ratios in the ^{Med}LHb. This effect was absent in the lateral aspect of the LHb (^{Lat}LHb), and occluded by naloxone and spontaneous MORwd (Fig. 2f,g; Supplementary Fig. 3a). TNF-α release may arise from microglial Toll-like receptor 4 (TLR4) signaling[10]. Systemically activating TLR4 with the agonist monophosphoryl lipid A (MPLA) in morphine-treated mice, instead of naloxone, mimicked MORwd plasticity (Supplementary Fig. 3b). Moreover, MPLA application in slices obtained from morphine-treated animals reduced AMPAR currents in the ^{Med}LHb, but not the ^{Lat}LHb (Supplementary Fig. 3c–d). MPLA-driven EPSC reduction did not occur in the presence of a dominant-negative peptide that blocks the soluble form of TNF-α[8] (XENP1595; Supplementary Fig. 3e). Furthermore, MORwd occluded MPLA-driven synaptic depression (Supplementary Fig. 3c), and systemic injection of XENP1595 prevented MORwd-induced plasticity (Supplementary Fig. 3f). Altogether, these results support the notion that TLR4 is expressed within the LHb (see the Allen Brain Atlas) and that its effect on AMPARs occurs via TNF-α signaling. Moreover, the results support the necessity and sufficiency of TNF-α for MORwd-driven reduction of LHb glutamatergic transmission.

TNF-α triggers its central effects partly through TNF receptor 1 (TNF-R1; encoded by *Tnfr1* (also known as *Tnfrsf1a*))[11]. We employed 129-Tnfrsf1atm3GkI (referred to as $Tnfr1^{fl/fl}$) mice in which *Tnfr1* expression in LHb neurons was knocked down via adenovirus (AAV)-Cre (Fig. 3a–c). After viral injection, AAV-Cre-$Tnfr1^{fl/fl}$ mice failed to show MORwd-driven AMPAR/NMDAR ratio reduction compared to AAV-Control-infused mice (Fig. 3d). This highlights the necessity of neuronal TNF-R1 for MORwd-driven depression of synaptic AMPARs in the LHb.

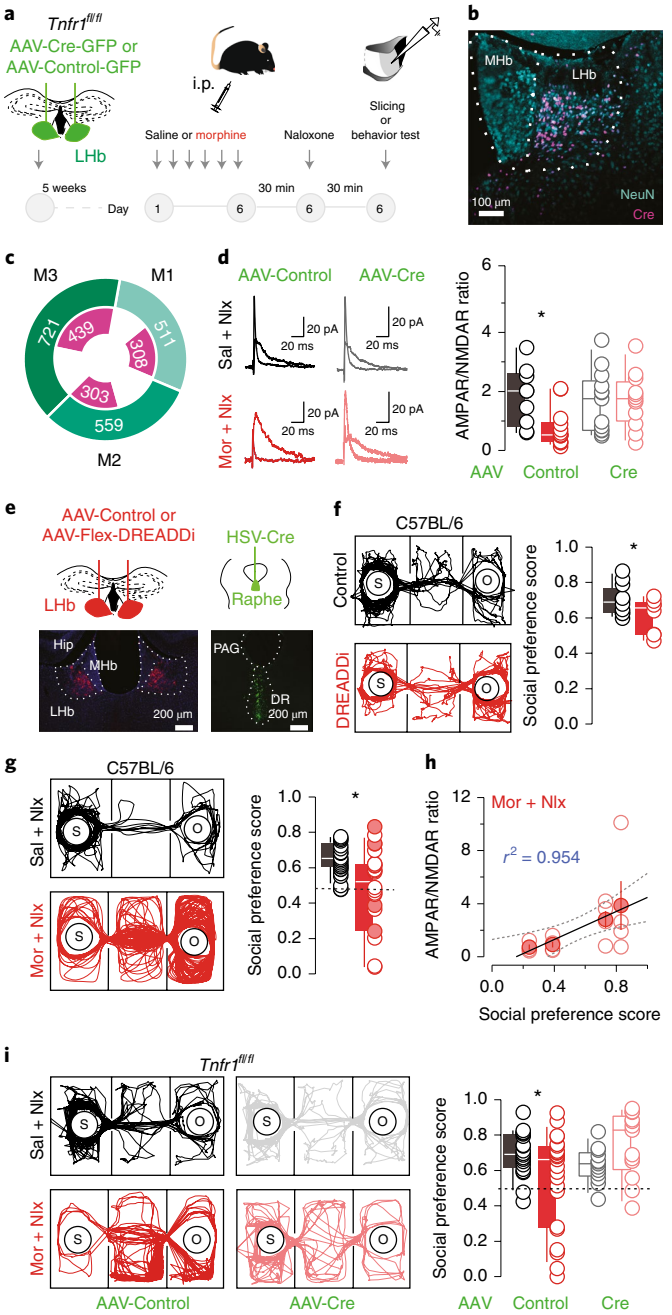

Fig. 3 | TNF-R1 requirements for MORwd-driven synaptic and behavioral adaptations. a, Experimental protocol. **b**,**c**, Image (**b**) and quantification (**c**) of AAV-Cre-infected LHb neurons (magenta) and total LHb neurons (cyan; 3 mice: M1, M2 and M3; NeuN, neuronal marker). **d**, Traces and AMPAR/NMDAR ratios from ^{Med}LHb of AAV-Control-*Tnfr1*$^{fl/fl}$ (saline + naloxone ($n = 2$ mice, 9 cells) versus NP-MORwd ($n = 3$ mice, 14 cells)) or AAV-Cre-*Tnfr1*$^{fl/fl}$ (saline + naloxone ($n = 4$ mice, 13 cells) versus NP-MORwd ($n = 3$ mice, 12 cells)). Interaction factor $F_{(1,44)} = 4.887$, two-way ANOVA, $^{*}P = 0.032$. **e**, AAV-Control or AAV-Flex-DREADDi virus injections in the LHb and HSV-Cre virus in the raphe (DR, dorsal raphe; Hip, hippocampus). **f**, Tracking plots and box and scatter plots of social preference test (SPT) in C57BL/6 mice expressing or not expressing DREADDi in LHb-to-raphe neurons (control virus versus DREADDi; $n = 8$ mice per group, $t_{18} = 2.271$, $^{*}P = 0.043$). **g**, Tracking plots of SPT in C57BL/6 mice. Box and scatter plots showing social preference score (saline + naloxone versus NP-MORwd; $n = 22$ mice per group, $t_{42} = 2.559$, $^{*}P = 0.014$). Filled circles indicate mice used for recordings in **h**. **h**, Correlation of AMPAR/NMDAR ratios and social preference score ($n = 4$ mice, 12 cells; Pearson's $r^2 = 0.954$, $^{*}P = 0.023$. Filled circles represent single cell; open circles represent average per mouse (mean and s.e.m.). **i**, Tracking plots and box and scatter plots of SPT in *Tnfr1*$^{fl/fl}$ mice (AAV-Control: saline + naloxone ($n = 20$ mice), NP-MORwd ($n = 20$ mice); AAV-Cre: saline + naloxone ($n = 13$ mice per group), NP-MORwd ($n = 13$ mice per group). Interaction factor $F_{(1,65)} = 7.20$, two-way ANOVA, $^{**}P = 0.009$. O, object, S, social stimulus. Data are presented as box plots, with 10th and 90th percentiles, median and scatter.

MORwd drives negative symptoms, including social detachment[1]. Similarly, LHb dysfunction contributes to the negative states emerging in addiction; however, the implications of LHb dysfunction with respect to sociability remains poorly addressed. We examined the contribution of the LHb-to-raphe pathway, the locus of MORwd plasticity, in social behavior. We employed an intersectional chemogenetic approach to reduce the efficiency of the LHb-to-raphe projection. This involved the combined retrograde expression of Cre-recombinase (HSV-Cre) in the dorsal raphe with the Cre-dependent expression of hM4Di (rAAV-hM4Di-mCherry, DREADDi) in the LHb (Fig. 3e). Reducing LHb-to-raphe efficiency with clozapine-*N*-oxide diminished social preference (Fig. 3f); this result supports the concept that the LHb contributes to social behaviors.

Next, we recapitulated MORwd-driven reduction in social preference in C57BL/6 mice (Fig. 3g; Supplementary Fig. 4a–d). Slices obtained from mice subjected to MORwd and exhibiting low or high sociability scores showed that ^{Med}LHb AMPAR/NMDAR ratios were positively correlated with the social score (Fig. 3h). This indicates that reduced synaptic strength in the LHb predicts opiate-withdrawal-driven sociability deficits.

Notably, microglia and TNF-α signaling also contributes to social behaviors[12]. Accordingly, MORwd-driven sociability deficits were absent after Cre-dependent LHb *Tnfr1* knockdown (Fig. 3i; Supplementary Fig. 4e–i). This genetic intervention did not affect locomotion (Supplementary Fig. 4j).

We found that MORwd-driven TNF-α release requires neuronal TNF-R1 to reduce AMPAR transmission onto raphe-projecting, medially located, LHb neurons. This ultimately gates MORwd-driven social impairment, a negative symptom typical of opiate withdrawal.

Together with sociability deficits, MORwd also leads to anxiety and hyperalgesia[1]. Since the contribution of the LHb on these two behavioral aspects remains elusive, we cannot rule out that MORwd-driven habenular plasticity is specific for withdrawal-mediated sociability defects.

The TNF-α–TNF-R1 engagement within the LHb represents a previously unidentified mechanism underlying precise cellular and behavioral aspects of MORwd. However, this is consistent with the following data: (1) drugs and drug-withdrawal-mediated modulation of AMPAR transmission partly rely on cytokine signaling[8]; (2) inhibition of TLR4 attenuates MORwd symptoms[13]; and (3) TNFRs contribute to social behaviors[14]. Notably, in pyramidal neurons of the hippocampus and cortex, TNF-α regulates AMPAR surface expression[15,16]. This phenomenon is opposite at striatal synapses where, similar to the LHb, TNF-α application results in decreased AMPAR transmission[8]. This divergence may arise from different TNF-α release dynamics, TNFR expression and signaling, or, alternatively, AMPAR anchoring properties within the LHb. MORwd modifies the morphology of microglia in the LHb. This is, at least partly, consistent with previous findings[8], yet it remains correlative with respect to TNF-α levels. This heightens the need to fill the gap in understanding regarding microglia function and its relationship with TNF-α within the habenula. Overall, while pharmacotherapies targeting pro-inflammatory pathways in substance abuse are missing, our data support cytokine signaling as a cellular pillar for aspects of drug addiction.

MORwd-driven TNF-α-dependent depression of AMPAR transmission occurs at LHb_{Raphe} neurons. From a circuit standpoint, this may provide an 'antisocial' signal that is likely produced through reduced actions onto raphe neuronal populations. This is consistent with the evidence reported here that chemogenetic manipulation of the LHb-to-raphe projection diminishes sociability. In addition, dopamine-containing and serotonin-containing raphe neurons contribute to social behaviors, and medially located LHb neurons monosynaptically connect to the latter[17–19]. Understanding the repercussions of LHb activity onto raphe neuronal subtypes during MORwd remains an important aspect for future investigation.

In conclusion, our data support the concept that cytokine-mediated plasticity participates in opiate-evoked negative symptoms, a mechanism by which the LHb ultimately contributes to the addiction spiral.

Online content

Any methods, additional references, Nature Research reporting summaries, source data, statements of code and data availability and associated accession codes are available at https://doi.org/10.1038/s41593-019-0421-4.

Received: 18 October 2018; Accepted: 7 May 2019;
Published online: 17 June 2019

References

1. Goeldner, C. et al. *Biol. Psychiatry* **69**, 236–244 (2011).
2. Lutz, P. E. et al. *Neuropsychopharmacology* **39**, 2694–2705 (2014).
3. Meye, F. J., Trusel, M., Soiza-Reilly, M. & Mameli, M. *Pharm. Biochem. Behav.* **162**, 87–93 (2017).
4. Margolis, E. B. & Fields, H. L. *PLoS One* **11**, e0159097 (2016).
5. Wang, J. et al. *Neurosci. Lett.* **653**, 64–70 (2017).
6. Valentinova, K. & Mameli, M. *Cell Rep.* **16**, 2298–2307 (2016).
7. Pollak Dorocic, I. et al. *Neuron* **83**, 663–678 (2014).
8. Lewitus, G. M. et al. *Neuron* **90**, 483–491 (2016).
9. Campbell, L. A., Avdoshina, V., Rozzi, S. & Mocchetti, I. *Brain Behav. Immun.* **34**, 130–140 (2013).
10. Michaud, M. et al. *J. Am. Med. Dir. Assoc.* **14**, 877–882 (2013).
11. Probert, L. *Neuroscience* **302**, 2–22 (2015).
12. Nie, X. et al. *Neuron* **99**, 464–479.e7 (2018).
13. Hutchinson, M. R. et al. *Brain Behav. Immun.* **22**, 1178–1189 (2008).
14. Patel, A., Siegel, A. & Zalcman, S. S. *Brain Behav. Immun.* **24**, 1276–1280 (2010).
15. He, P., Liu, Q., Wu, J. & Shen, Y. *FASEB J.* **26**, 334–345 (2012).
16. Stellwagen, D., Beattie, E. C., Seo, J. Y. & Malenka, R. C. *J. Neurosci.* **25**, 3219–3228 (2005).
17. Kane, M. J. et al. *PLoS One* **7**, e48975 (2012).
18. Lecca, S. et al. *eLife* **6**, e30697 (2017).
19. Matthews, G. A. et al. *Cell* **164**, 617–631 (2016).

Acknowledgements

The authors thank F.J. Meye and the Mameli Laboratory for comments on the manuscript. This work was supported by funds from the ERC StG SalienSy 335333 and the SNSF (31003A) to M.M. They also thank D. Szymkowski for the donation of XENP1595, and G. Kollias and H. Strubbe for the use and breeding of the *Tnfr1*$^{fl/fl}$ mouse line.

Author contributions

K.V., A.T. and M.M. performed and analyzed the ex vivo recordings and behavior experiments. A.L.L. and J.A.C. contributed to the ex vivo recordings. M.T., I.M. and L.M. performed the molecular biology experiments. C.B. and S.T. provided support for the behavioral experiments. A.M. and R.C.P. analyzed the microglia morphology. A.V. provided conceptual and experimental input related to TNF-α signaling and the *Tnfr1*$^{fl/fl}$ mice. K.V. and M.M. conceptualized, designed the study and wrote the manuscript.

Competing interests

The authors declare no competing interests.

Additional information

Supplementary information is available for this paper at https://doi.org/10.1038/s41593-019-0421-4.

Reprints and permissions information is available at www.nature.com/reprints.

Correspondence and requests for materials should be addressed to M.M.

Journal peer review information: *Nature Neuroscience* thanks David Stellwagen and the other, anonymous, reviewer(s) for their contribution to the peer review of this work.

Publisher's note: Springer Nature remains neutral with regard to jurisdictional claims in published maps and institutional affiliations.

Methods

Animals and morphine treatment. C57BL/6J wild-type mice (male) and 129-Tnfrsf1atm3GkI mice (male and female, referred to as *Tnfr1*$^{fl/fl}$) aged 4–10 weeks were group-housed (three to five per cage) on a 12–12 h light cycle (lights on at 7:00) with food and water ad libitum. All procedures aimed to fulfill the criterion of the 3Rs and were approved by the Veterinary Offices of Vaud (Switzerland; license VD3172). Part of the current study was carried out at the Institut du Fer a Moulin, Paris, France, and experiments were performed in accordance with the guidelines of the French Agriculture and Forestry Ministry. MORwd was either precipitated with naloxone or was induced naturally. For naloxone-precipitated MORwd, mice were subjected to intraperitoneal (i.p.) morphine (20 mg per kg, Cantonal Hospital of Lausanne, Switzerland) or saline injections (saline and morphine-treated animals were housed together) for 6 days. On day 6, the last morphine or saline injection was given in a separate cage. After 30 min, the animals then received an i.p. injection of naloxone hydrochloride (2 mg per kg, Abcam). MORwd-dependence symptoms were allowed to develop in the following 30 min, after which the mice were either killed for ex vivo electrophysiological recordings or were subjected to behavioral tests.

For spontaneous withdrawal, mice were treated with morphine or saline for 6 days and were killed for recording experiments 10–13, 20 or 30 days after the last injection. For recordings in morphine-treated animals not in withdrawal, mice were killed 1 h after the last morphine injection on day 6. To assess for the involvement of TNF-α in MORwd plasticity, some of the animals were subjected to an i.p. injection of MPLA (10 µg, dissolved in dimethylsulfoxide (DMSO) and saline) or saline (containing the same amount of DMSO as control)[8] instead of naloxone 30 min after the last morphine injection on day 6. Another group of the animals received an i.p. injection (30 mg per kg) of a dominant-negative peptide blocking the soluble form of TNF-α (XENP1595, Xencor)[8] 1 h before the last morphine or saline injection on day 6. Thirty minutes after the morphine or saline injection, these animals received naloxone and were killed for recording experiments as described above. No statistical methods were used to predetermine sample sizes, but our sample sizes were similar to previously reported numbers[6].

Surgery. Animals of at least 4 weeks of age were anesthetized with an i.p. injection of ketamine (150 mg per kg)/xylazine (100 mg per kg; veterinary office the University of Lausanne) and were placed on a stereotactic frame (Kopf). Bilateral injections of 200–400 nl were performed through a glass needle at a rate of approximately 100 nl min^{-1}. The injection pipette was withdrawn from the brain 10 min after the infusion. Retrobeads (Lumafluor) were infused into the dorsal raphe nucleus (anterior–posterior (AP): −3.5 mm; medial–lateral (ML): 0 mm; dorsal–ventral (DV): −3.8 mm) or the VTA (AP: −2.4 mm; ML: ±0.65 mm; DV: −4.9 mm) of C57BL/6 mice. *Tnfr1*$^{fl/fl}$ mice were injected with either rAAV2-hSyn-eGFP or rAAV2-hSyn or CMV-Cre-eGFP into the LHb (AP: −1.35 mm; ML: ±0.45 mm; DV: −3.00 mm). In another set of experiments, C57BL/6 mice were injected with a herpes simplex virus-derived hEF1α-Cre vector (MGA Gene Delivery Technology Core) in the raphe nucleus and with rAAV-DJ-EF1α-Flex-hM4D(Gi)-mCherry (Gene Vector and Virus Core, Stanford Medicine) in the LHb. Animals were allowed to recover for about 5–7 days after injection of the retrobeads or 5 weeks after viral infusion before being treated with morphine or saline. The injection sites were carefully examined during all electrophysiology experiments, and only animals with correct injections were used for recordings. Similarly, for behavioral studies, only animals with correct injection sites were included in the analyses. Brain slices obtained from mice injected with retrobeads or viruses were directly examined under an epifluorescence microscope.

Ex vivo electrophysiology. Animals aged 5 weeks were anesthetized with an injection of ketamine (150 mg kg)/ xylazine (100 mg/kg) for preparation of LHb-containing brain slices. Slicing was done in bubbled ice-cold 95% O_2/5% CO_2-equilibrated solution containing (in mM): 110 choline chloride, 25 glucose, 25 $NaHCO_3$, 7 $MgCl_2$, 116 ascorbic acid, 3.1 sodium pyruvate, 2.5 KCl, 1.25 NaH_2PO_4, and 0.5 $CaCl_2$. Coronal slices (25 µm) were prepared and transferred for 10 min to warmed solution (34 °C) of identical composition before they were stored at ~22 °C in 95% O_2/5% CO_2-equilibrated artificial cerebrospinal fluid containing (in mM): 124 NaCl, 26.2 $NaHCO_3$, 11 glucose, 2.5 KCl, 2.5 $CaCl_2$,1.3 $MgCl_2$, and 1 NaH_2PO_4. Recordings (flow rate of 2.5 ml min^{-1}) were obtained using an Olympus-BX51 microscope (Olympus) at 32 °C. Patch-clamp experiments were performed using borosilicate glass pipettes (2.7–4 MΩ; Phymep). Currents were amplified, filtered at 5 kHz and digitized at 20 kHz (Multiclamp 200B; Molecular Devices). Data were acquired using Igor Pro with NIDAQ tools (Wavemetrics). Access resistance was monitored by a step of −4 mV (0.1 Hz). Experiments were discarded if the access resistance increased by more than 20%. All recordings were made in voltage-clamp configuration. Spontaneous EPSCs were recorded either in the ^{Lat}LHb or ^{Med}LHb at −60 mV in the presence of picrotoxin (100 µM; Abcam) and APV ((2R)-amino-5-phosphonovaleric acid, 50 µM, Abcam). The internal solution contained (in mM): 130 CsCl, 4 NaCl, 2 $MgCl_2$, 1.1 ethylene glycol tetraacetic acid (EGTA), 5 HEPES buffer, 2 ATP-Na_2, 5 sodium creatine-phosphate, 0.6 GTP-Na_3, and 0.1 spermine. The liquid junction potential was −3 mV and was not compensated. For determining the AMPAR/NMDAR ratios, EPSCs were evoked through glass electrodes placed ~200 µm from the recording site using an AMPI ISO-Flex stimulator. A mixture of AMPA and NMDA currents were evoked at +40 mV (in the presence of picrotoxin). The two components were pharmacologically isolated by adding APV in the recording solution and by subsequent identification of the individual currents via digital subtraction. For glutamate uncaging experiments, MNI-glutamate (4-methoxy-7-nitroindolinyl-caged L-glutamate, 500 µM; Tocris) was added to the recording solution. Uncaging was obtained via a single-path photolysis head (Prairie Technologies) connected to a solid-state laser (Rapp Optolectronics; 405 nm, duration 1 ms, diameter 3–5 µm, 250–300 µm from the soma). AMPAR/NMDAR ratios in uncaging experiments were calculated as follows: AMPA-EPSCs at −60 mV/NMDA-EPSCs at +40 mV. The individual components were identified as previously described[6], using the late component of the EPSC at 30 ms after the onset. The rectification index was computed by recording AMPA-EPSCs at −70 mV and +40 mV and was calculated as follows: (AMPA-EPSC at −70/AMPA-EPSC at +40)/1.75. To assess presynaptic release properties, trains of AMPAR-EPSCs were evoked using an extracellular-stimulating electrode (5 pulses at 5 Hz, 10 Hz and 20 Hz). The amplitudes of EPSC trains were normalized to the amplitude of the first pulse. When indicated, recordings were performed from retrogradely labeled and fluorescently identified LHb neurons. Some experiments were performed in LHb-containing slices incubated for a minimum of 1 h with exogenous TNF-α (100 ng ml^{-1}). To test the effect of MPLA on AMPAR transmission, neurons were patched either in the ^{Lat}LHb or the ^{Med}LHb, and EPSCs were evoked with extracellular stimulation. Following a 10-min baseline, MPLA (1 µg ml^{-1}) was added to the recording solution and EPSCs were recorded for a minimum of 40 min. Some experiments were performed in the presence of the TNF-α dominant-negative peptide XENP1595 (6 mg 1 ml^{-1}; Xencor) in the recording solution.

Non-stationary fluctuation analysis. A peak-scaled non-stationary fluctuation analysis was performed on sEPSCs (number of events, 70–250) (Synaptosoft). sEPSCs were selected by applying the following criteria: fast rise time alignment, stable baseline holding current and the absence of spurious fluctuations during the sEPSC decay. The variance–amplitude relationship of sEPSC decay was plotted and fitted with the equation $\sigma^2 = iI - I^2/N + \sigma_b^2$ (where i is the mean single-channel AMPA current, I is the mean current, N is the number of channels activated at the peak, N = mean amplitude/i; and σ_b^2 is the baseline variance). i was estimated as the slope of the linear fit of the first portion of the parabola of the fitted sEPSC decay. The goodness-of-fit was assessed with a least-squares algorithm. The unitary current was converted into conductance based on the reversal potential of evoked EPSCs (~0 mV) and the holding potential (−60 mV). Conductance and average EPSC amplitude, mean rise time, mean decay time, access resistance or background noise variance had no correlation ($P > 0.4$).

Histology and immunofluorescence. Mice were injected daily with saline or morphine (20 mg per kg, i.p.) for 6 days. Some mice were left to develop spontaneous withdrawal, while others received naloxone (2 mg per kg, i.p.) injection 30 min after the last saline or morphine injection on day 6. After 10–13 days of spontaneous withdrawal or 30 min after naloxone injection, mice were anesthetized and perfused with cold 4% paraformaldehyde (PFA) in PBS. The brains were extracted, post-fixed in 4% PFA in PBS and then incubated in 30% sucrose in PBS until they sank. Slices (30 µm) were cut using a cryostat and stored in PBS containing 0.02% NaN_3 for future analyses. For immunofluorescence, the slices were incubated for 2 h in blocking buffer (5% NGS (normal goat serum), 0.3% Triton-X in PBS) and then incubated for 24 h at 4 °C with the primary antibody solution (mouse anti-TNF-α antibody, 1:100 in blocking buffer; ab1793, Abcam)[8]. After extensive rinses, the secondary antibody was applied (goat anti-mouse IgG-conjugated Alexa 488, Invitrogen, 1:400 in blocking buffer, 24 h at 4 °C). The slices were then incubated in 4,6-diamidino-2-phenylindole (DAPI) (1:400 solution in PBS), extensively rinsed, mounted on glass slides with Pro-Long Gold Antifade Reagent (Invitrogen) and coverslipped. Images were acquired with an epifluorescence microscope with a ×20 objective (AxioVision, Zeiss) using the same parameters for all the samples. The images were analyzed and processed using the software ImageJ. Optical density was measured on the whole LHb area and normalized against the neighboring thalamus using the following equation: LHb – thalamus/(LHb + thalamus). A total of three to six slices distributed in the rostrocaudal axis were analyzed per animal (eight morphine-treated, seven saline-treated).

Microglia analysis. Mice were anesthetized and perfused with cold 4% PFA in PBS. The brains were extracted, post-fixed in 4% PFA in PBS and then incubated in 30% sucrose in PBS until they sank. Slices (30 µm) were cut using a cryostat and stored in PBS containing 0.02% NaN_3 for future analyses. Brain sections were permeabilized at room temperature in 0.5% Triton X-100 (Sigma) for 1 h at room temperature, followed by blocking in 2% BSA 0.5% Triton X-100 for 1 h at room temperature and then overnight incubation with primary antibody (IBA1, 1:1,000 (cat. no. 019–19741, Wako Chemicals) and CD68, 1:400 (cat. no. MCA1957, Bio-Rad))[8] at 4 °C. After washing, sections were incubated for 2 h at room temperature with Alexa-fluorophore-conjugated secondary antibodies (Invitrogen) and counterstained with DAPI (Invitrogen).

Confocal microscopy was performed using a TCS-SP5 (Leica) Laser Scanning System with a ×20 dry objective. Images were processed and analyzed using the software Fiji or Imaris (Bitplane) as appropriate. Imaris was used for three-dimensional (3D) rendering of confocal images for quantification of volumes.

For density analyses, for each acquisition, the DAPI channel was max-projected and the ^{Med}LHb and ^{Lat}LHb were manually drawn as regions of interest. Then, stacks ranging from 15 µm to 20 µm in thickness, with a *z*-step size of 1 µm, were processed as follows: IBA1 and DAPI channels were thresholded in Fiji and multiplied to each other for each stack, with the image calculator function. The resulting thresholded stack was max-projected, and the microglia nuclei were counted using the function Analyze Particle.

For cell soma size and IBA1 intensity analyses, each acquisition was max-projected, and the contour of cell somata in the ^{Med}LHb were manually drawn based on the immunoreactivity of IBA1 and then analyzed per size in µm^2 and intensity.

3D imaging analysis was performed using Imaris and applying recorded algorithms (fixed thresholds for signal intensity) to all the images of the same experiment to produce unbiased signal quantification. In each experiment, one brain slice per animal ($n=4$) per group was acquired. The microglial cell volume and the volume of phagocytic structures were reconstructed based on the absolute intensity of IBA1 and CD68 signals, respectively. The volume of CD68 was then normalized to the IBA1 volume to take in account the cell size.

Behavior. *Social preference test.* A three-chambered social preference test was used. The arena was a rectangular Plexiglas (60 × 40 × 22 cm) (Ugo Basile) divided into three chambers. The walls of the center chamber had doors to allow free access to all compartments. The luminosity was around 10 lux. Thirty minutes after naloxone injection, each mouse was placed in the arena for a habituation period of 10 min and was allowed to freely explore the whole empty arena. The social preference test was performed immediately after the end of the habituation period: two enclosures with vertical bars were placed in the middle of the two lateral compartments, while the central chamber remained empty. One enclosure was empty (serving as an inanimate object), whereas the other contained a social stimulus (an unfamiliar juvenile mouse 25 ± 1 days old). The enclosures allowed visual, auditory, olfactory and tactile contact between the experimental mice and the social stimuli mice. The juvenile mice in the enclosures were habituated to the apparatus and the enclosures for 3 days before the experiment, and each one of them served as a social stimulus for no more than 2 experimental mice (at least 6 weeks old). The test lasted 10 min, whereby the experimental mice were allowed to freely explore the apparatus and the enclosures. The position of the empty and juvenile-containing enclosures alternated and was counterbalanced for each trial to avoid any bias effects. Every session was video-tracked and recorded using Ethovision XT (Noldus) or AnyMaze (Stoelting), which provided an automated recording of the entries and time spent in the compartments, the distance moved and the velocity. The time spent in each chamber was assessed and then used to determine the preference score for the social compartment as compared to the object compartment (social/(social + object)). The arena was cleaned with 1% acetic acid solution and dried between trials.

Analyses and statistics. Animals were randomly assigned to experimental groups. Compiled data are reported and presented as whisker box plots (the upper and lower whiskers representing the 90th and 10th percentiles, respectively, and the upper and lower boxes representing the 75th and 25th percentiles, respectively, and the horizontal line representing the median) or the mean ± s.e.m., with single data points plotted (single cell for electrophysiology and single animal for behavioral experiments). Animals or data points were not excluded unless stated, and a normality test was applied. Data collection and analyses were not performed blinded to the conditions of the experiments. When applicable, statistical tests were paired or unpaired *t*-test and one-way or two-way analysis of variance (ANOVA). Significance for correlations was obtained applying Pearson's estimates. Testing was always performed two-tailed with $\alpha=0.05$. More information on the methods and analyses can be found in the Nature Research Reporting Summary.

Reporting Summary. Further information on research design is available in the Nature Research Reporting Summary linked to this article.

Data availability

The datasets generated during and/or analyzed during the current study are available from the corresponding author upon reasonable request.

nature research

Corresponding author(s): Manuel Mameli

Last updated by author(s): April 16 2019

Reporting Summary

Nature Research wishes to improve the reproducibility of the work that we publish. This form provides structure for consistency and transparency in reporting. For further information on Nature Research policies, see Authors & Referees and the Editorial Policy Checklist.

Statistics

For all statistical analyses, confirm that the following items are present in the figure legend, table legend, main text, or Methods section.

n/a	Confirmed	
☐	☒	The exact sample size (*n*) for each experimental group/condition, given as a discrete number and unit of measurement
☐	☒	A statement on whether measurements were taken from distinct samples or whether the same sample was measured repeatedly
☐	☒	The statistical test(s) used AND whether they are one- or two-sided *Only common tests should be described solely by name; describe more complex techniques in the Methods section.*
☒	☐	A description of all covariates tested
☐	☒	A description of any assumptions or corrections, such as tests of normality and adjustment for multiple comparisons
☒	☐	A full description of the statistical parameters including central tendency (e.g. means) or other basic estimates (e.g. regression coefficient) AND variation (e.g. standard deviation) or associated estimates of uncertainty (e.g. confidence intervals)
☐	☒	For null hypothesis testing, the test statistic (e.g. *F*, *t*, *r*) with confidence intervals, effect sizes, degrees of freedom and *P* value noted *Give P values as exact values whenever suitable.*
☒	☐	For Bayesian analysis, information on the choice of priors and Markov chain Monte Carlo settings
☒	☐	For hierarchical and complex designs, identification of the appropriate level for tests and full reporting of outcomes
☐	☒	Estimates of effect sizes (e.g. Cohen's *d*, Pearson's *r*), indicating how they were calculated

Our web collection on statistics for biologists contains articles on many of the points above.

Software and code

Policy information about availability of computer code

Data collection	Data were acquired with commercially available softwares indicated in the Methods section: IGOR Wavemetrics, Anymaze Stoelting, Ethovision XT, AxioVision Zeiss.
Data analysis	Data were analyzed with commercially available softwares indicated in the Methods section: IGOR Wavemetrics, Anymaze Stoelting, Graphpad Prism, Imaris, ImageJ and Fiji Plugin.

For manuscripts utilizing custom algorithms or software that are central to the research but not yet described in published literature, software must be made available to editors/reviewers. We strongly encourage code deposition in a community repository (e.g. GitHub). See the Nature Research guidelines for submitting code & software for further information.

Data

Policy information about availability of data

All manuscripts must include a data availability statement. This statement should provide the following information, where applicable:

- Accession codes, unique identifiers, or web links for publicly available datasets
- A list of figures that have associated raw data
- A description of any restrictions on data availability

The data sets generated during and/or analysed during the current study are available from the corresponding author on reasonable request.

Field-specific reporting

Please select the one below that is the best fit for your research. If you are not sure, read the appropriate sections before making your selection.

☒ Life sciences ☐ Behavioural & social sciences ☐ Ecological, evolutionary & environmental sciences

Life sciences study design

All studies must disclose on these points even when the disclosure is negative.

Sample size	Sample size was based on the based of previous results obtained in the laboratory. This is based on the specific variance observed in the region of interest studied. This is now stated in the methods with a reference of our previously published work
Data exclusions	The methods include an exclusion criteria related to the quality of the recording (access resistance) which reflects the physiological parameters of recorded neurons and site of injection in the surgery section which was always controlled.
Replication	Each experiment was replicated at minimum three times.
Randomization	Animals were randomly assigned to experimental groups.
Blinding	The operators were not blind of the experimental groups in the case of ex-vivo recordings. Double control with the PI and peers in the lab, as well cross controlled recordings within the laboratory allow the operator to not be blind of the experimental condition with no risk in biasing the result. The experimenters were blind for the analysis of the behavioral and immunolabeling experiments.

Reporting for specific materials, systems and methods

We require information from authors about some types of materials, experimental systems and methods used in many studies. Here, indicate whether each material, system or method listed is relevant to your study. If you are not sure if a list item applies to your research, read the appropriate section before selecting a response.

Materials & experimental systems

n/a	Involved in the study
☐	☒ Antibodies
☒	☐ Eukaryotic cell lines
☒	☐ Palaeontology
☐	☒ Animals and other organisms
☒	☐ Human research participants
☒	☐ Clinical data

Methods

n/a	Involved in the study
☒	☐ ChIP-seq
☒	☐ Flow cytometry
☒	☐ MRI-based neuroimaging

Antibodies

Antibodies used	mouse anti-TNFα antibody, ab1793, clone number 52B83, Lot#GR66942 Abcam, 1:100 in blocking buffer goat anti-mouse IgG-conjugated Alexa 488, Catalog # A28175, Lot#1874804 (No clone# available), Invitrogen, 1:400 in blocking buffer, 24h at 4°C Iba1 1:1000, Wako Chemicals, Cat. 019-1974 Clone NCNP24, Lot. PTN5930 CD68 1:400, Bio-Rad Cat. MCA1957, Clone FA-11, Lot. 1807
Validation	mouse anti-TNFα antibody validation was based on published results from Lewitus et al., 2016. This is now stated in the manuscript, methods session. Iba1 and CD68 validation was based on previous publication including Lewitus et al., 2016 and Paolicelli et al., 2011. Dr. Paolicelli is an authors of this manuscript therefore the validation of these antibodies were based on her experience in the field. The entire validation reported here is valid for the species used in this study which is mice.

Animals and other organisms

Policy information about studies involving animals; ARRIVE guidelines recommended for reporting animal research

Laboratory animals	C57Bl/6J wild-type (male) and 129-Tnfrsf1atm3Gkl (male and female, referred as TNF-R1fl/f) mice of 4–10 weeks were used
Wild animals	This study did not involve the use of wild animals
Field-collected samples	This study did not involve the use of field collected samples
Ethics oversight	All procedures were approved by the Veterinary Offices of Vaud (Switzerland; License VD3172)

Note that full information on the approval of the study protocol must also be provided in the manuscript.